

A fibre-optic displacement sensor for a cyclotron environment based on a modified triangulation method

Jovan Elazar¹, Sandra Šelmić², Miloš Tomić and Milan Prokin

Faculty of Electrical Engineering, University of Belgrade, PO Box 35-53,
Belgrade 11120, Serbia

E-mail: sselmic@latech.edu

Received 1 May 2002, in final form 10 July 2002

Published 4 November 2002

Online at stacks.iop.org/JOptA/4/S347

Abstract

Due to the very high magnetic and radio frequency fields and generally hostile environment inside cyclotrons, electronic devices are hindered from functioning. By implementing a modified triangulation method we developed a purely dielectric PC interfaced sensor head, which will be placed inside the cyclotron for electrode-position measurement. This represents a completely new cyclotron diagnostic tool designed to cope with cyclotron alignment problems. In this paper we present the motivations for developing such a sensor, the theoretical analysis, overall sensor design for two-coordinate simultaneous measurement and measurement results. A resolution of 10 μm within a 5 mm range was achieved independently of laser diode power variation, target reflectance variation and induced attenuation in optical fibres.

Keywords: Sensor, optical distance measurement, optical fibre applications

(Some figures in this article are in colour only in the electronic version)

1. Introduction

The displacement and consequent misalignment of electrodes in cyclotron is a problem which has been carefully studied [1, 2]. It can cause degradation of ion-beam intensity and quality. The loss of an ion beam in the central region of the cyclotron, where ions are at low energies, affects only the overall efficiency of the machine. The ion-beam loss closer to the extraction region, in addition to reducing the machine's efficiency, induces significant radioactivity in the cyclotron components. This is particularly true for proton beams because they make a large number of turns in the machine and the level of radioactivity induced by high-energy protons is higher than with other ions. The importance of ion-beam quality becomes even more pronounced when the

cyclotron is used as an injector to a second accelerator, when the ion-beam emittance, momentum, and dispersion have to be matched precisely with the input parameters of the second accelerator [3].

We have developed a completely new cyclotron diagnostics for measuring electrode displacement. It is a fibre-optic displacement sensor, compatible with the cyclotron environment, which is expected to help cope with the misalignment problems: to get the ion beams out of the cyclotron in the running-up period of the cyclotron and to improve the cyclotron performance later on.

After evaluating many optical measuring methods, we decided to modify the optical triangulation by separating the sensor head from the electronics. We designed a completely dielectric and passive sensor head, which can be placed inside the cyclotron. The electronics are positioned outside of the cyclotron and out of reach of its hostile environment. The electronics are connected to the sensor head with optical fibres.

¹ Present address: Unit of Electrooptics Engineering, Ben-Gurion University of the Negev, PO Box 653, Beer-Sheva 84105, Israel.

² Present address: Institute for Micromanufacturing, Louisiana Tech University, PO Box 10137, Ruston, LA 71272, USA.

2. Motivation for the development of the electrodes displacement sensor

Modern multi-particle cyclotrons with variable ion energies can let the gap between the accelerating electrodes in the central region be as small as 10 mm, especially in the case of the commonly used dee-in-valley construction (cyclotron electrodes are traditionally called *dee* because their initial shape was in the form of the letter D). The need for high flutter and high magnetic circuit efficiency imposes an additional restriction on the vertical beam apertures of only 20–30 mm. This makes the alignment problem difficult. Small radio frequency (RF) gaps also increase the probability of sparking in the central region because the disturbed positions of the electrodes causes a reduction in the inter-electrodes gap values, which can bring the RF field above the Kilpatrick criterion [4].

There are several sources of misalignment in the cyclotron central region. Apart from fabrication imperfections, which can be corrected during the cyclotron assembly, vertical sag of the dee (in the case of cantilever stem-dee construction), thermal stress, magnetic forces, vibrations caused by the turbulence in the dee cooling water, and vacuum-induced stress imposed on the whole cyclotron chamber construction, can all contribute to the electrode misalignment. Translations of the dee tip in all three directions and twisting of the dee around the axis of the stem can be expected. It is hardly possible to calculate the overall misalignment because of the complexities of the mechanical construction, temperature distribution, and acting forces. Usually the effects are observed as ion-beam loss. For example, the TRIUMF RF resonators had to be redesigned because the motion of the dee tip caused by differential thermal expansion and water-flow-induced vibrations was approximately 2.5 mm [5]. The maximum change in the distance between the magnetic poles caused by a magnetic force on the Dubna U-400 cyclotron [6] was measured to be 2.5 mm.

The VINCY cyclotron [7, 8] is an isochronous machine with a 2 m pole diameter and a magnetic field of more than 2 T, two RF cavities of $\lambda/4$ type, and an overall stem-dee cantilever length of more than 3.7 m. The minimal RF gap in the central region is 10 mm in the horizontal and 30 mm in the vertical direction making the machine very sensitive to problems caused by misalignment. The maximal RF voltage of 100 kV and minimal radius of curvature of the dee tip of 6 mm contribute to the high sparking probability. Therefore, the dee support system of the VINCY RF cavities is equipped with a positioning mechanism that was three translational and one rotational degree of freedom to compensate for the dee misalignment. The positioning mechanism could not operate properly, if at all, unless the adequate sensing system, which will be able to determine the dee position with required accuracy, is provided. The measuring accuracy was set by the cyclotron constructors, taking into the account all the safety margins, to be 50 μm .

3. The overview of the possible sensor designs

There is no cyclotron with the dee position diagnostics anywhere in the world, although, because of the reasons mentioned above, the necessity for it is widely recognized in

the cyclotron community. It was clear from the very beginning that such a sensing system cannot be based on electronic or conductive components placed inside the cyclotron where high magnetic and RF fields will disable them from functioning. The photonic system imposed itself as the solution to the problem with all the electronic components safely displaced outside the reach of the scattered fields.

Although seemingly simple on first sight, measurement with a laser positioned outside the scattered magnetic field, at approximately 10 m from the centre of the cyclotron, was quickly disregarded as being unreliable. The typical value for the directional stability of a high-quality HeNe laser of 0.03 mrad will produce an error in the laser spot position at the target of 300 μm . Effects of vibrations of the cyclotron and strain induced on the optical window of the vacuum chamber, when the chamber is brought under vacuum, although not easily predictable, are considered to be even more severe impairments to the measurement accuracy. Therefore it was necessary to carry the optical signal from the laser to the place of measurement and the information about the target position back to an optical detector through optical fibres.

Various fibre-optical methods for distance measurement have been evaluated for dee position measurement inside the cyclotron [9–22]. Using an optical time domain reflectometer (OTDR) with interferometric detection technique, as well as an optical frequency domain reflectometer (OFDR), requires complex laser sources [11–14]. The fringe counting technique has resolution smaller than the wavelength, which would be more than enough for our application, and a wide measuring range, but there is a problem of measurement initialization. Also, there is a danger of losing the count due to the cyclotron vibrations. An optical low-coherence reflectometer (OLCR) has mechanically movable parts for interferometer arms optical length equalization, adding to the system complexity [15–17]. Another drawback of interferometric methods is their sensitivity to intensity and polarization change experienced by light during reflection from the target.

Geometrical methods with non-interferometric detection are also quoted in the literature [18–22]. None of them were found to be suitable for the dee-position measurements. Sometimes high resolution and dynamic range are unachievable together because there is a limitation in the total number of measuring points, i.e. the resolution is inversely proportional to the measuring range [18, 19]. The presence of electronic components makes some geometrical methods [12] unusable in a hostile environment. Other fibre-optic geometric methods are not compensated for the optical signal level change [21, 22], caused by both target reflectance change and radiation-induced fibre attenuation.

Optical triangulation is a well elaborated and inherently very simple and reliable optical method for measuring distance. It is widely used with the laser as the light source, both for specularly and diffusely reflecting targets. In both cases, the displacement of the target changes the position of the laser spot on the target and its image on the detector. A special optoelectronic device, called a position sensitive detector (PSD), was developed to facilitate distance measurements based on optical triangulation. It is a semiconductor detector, lengthy in shape, with two electrical connections at the ends and one at the middle. By performing

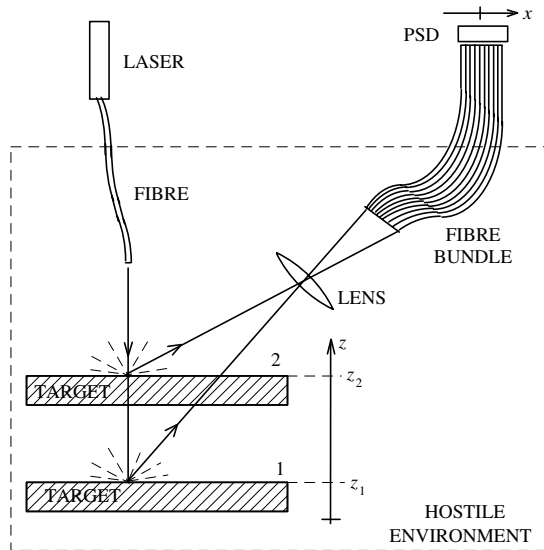


Figure 1. The modified optical triangulation method. The target is a diffusive reflector. A change in the target position along the z -direction causes movement in the light spot on the PSD along the x -direction. The example of two different target positions is shown.

some mathematical operations on the photocurrents from these three electrical connections, the position of the ‘centre of gravity’ of the light spot impinging on the detector can be determined. At the same time the influence of the change of the incident light flux on measurement accuracy can be eliminated. Unfortunately, the standard optical triangulation method cannot be employed for dee-position measurement because an optical source and detector cannot be put inside the cyclotron. If they are positioned outside the cyclotron, even if the laser beam directional instability is neglected, the extremely ‘narrow’ triangle geometry will be useless for any measurements.

4. Modified optical triangulation method

We modified the standard triangulation method using an optical fibre to guide the laser light to the place where the dee position has to be measured and used a coherent optical fibre bundle to relay the distribution of light reflected from the target back to the PSD. The target was a copper plate with a diffusely reflecting surface placed on the anti-dee surface. The laser, PSD and all electronics can be positioned outside the cyclotron, at a distance where magnetic and RF fields cannot interfere with their function. In that way we obtained a completely dielectric sensor head which can function in the cyclotron environment.

The basic principle of the modified optical triangulation with a diffusely reflecting target is shown in figure 1 [23]. Light from a laser diode is coupled to a multimode fibre and delivered to the sensor head. With a lens in the sensor head the light coming out of this fibre is projected onto the target. With another lens the light spot distribution on the target is imaged on the input face of a coherent optical fibre bundle.

In the coherent fibre bundle the optical fibres are carefully arranged so that every single fibre in the bundle has the same position on the input face of the bundle as on the output face.

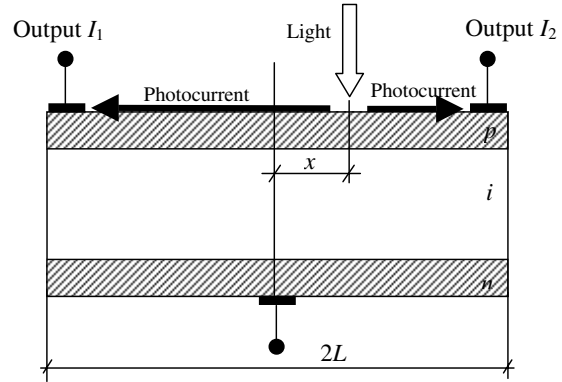


Figure 2. PSD sectional view.

In that way the light distribution can be relayed from the input face to the output face with the unavoidable degradation due to the discrete nature of the fibre bundle. With careful bundle design, which has to match the PSD sensitive surface in shape and size, this degradation in image quality can be kept within a tolerated level. The output face of the bundle is brought to close proximity of the PSD sensitive surface.

A photocurrent generated by the incident light is divided inside the PSD into two output currents, I_1 and I_2 , which flow through the electrical contacts at the ends of the PSD (see figure 2). These currents depend not only on the light flux, but also, which is essential for the measurement, on the position of the light spot along the PSD. By dividing the difference of currents I_2 and I_1 by the total current I , which flows through the middle contact of PSD and represents the sum of currents I_1 and I_2 , the position x of the light spot on PSD can be determined [24]

$$S = \frac{x}{L} = \frac{I_2 - I_1}{I} = \frac{I_2 - I_1}{I_2 + I_1}, \quad (1)$$

where L is the PSD half-length (see figure 2). We shall refer to the non-dimensional quantity S in further text as the PSD signal. By performing the division in equation (1), the dependence of currents I_1 and I_2 on the input light flux is cancelled out. In that way the PSD signal and the measurement performed with it are made independent of any changes in the input light flux.

5. Two coordinate fibre-optic displacement sensor

The design of the position measuring system based on the modified triangulation method can be adapted for two-dimensional measurement in the two orthogonal directions (y and z coordinates). This is achieved by using two diode lasers coupled to two separate fibres delivering light to the target. One of them illuminates a specially designed slanted part on the target. Time multiplexing laser operation enables the use of the same coherent fibre bundle, which is the most expensive part of the system, for measurement in both directions with only one PSD at the end. The same concept can be extended for simultaneous measurement of three coordinates (x , y and z).

The fibre-optic displacement sensor consists of the optical sensor head, coherent optical fibre bundle and electronics (figure 3).

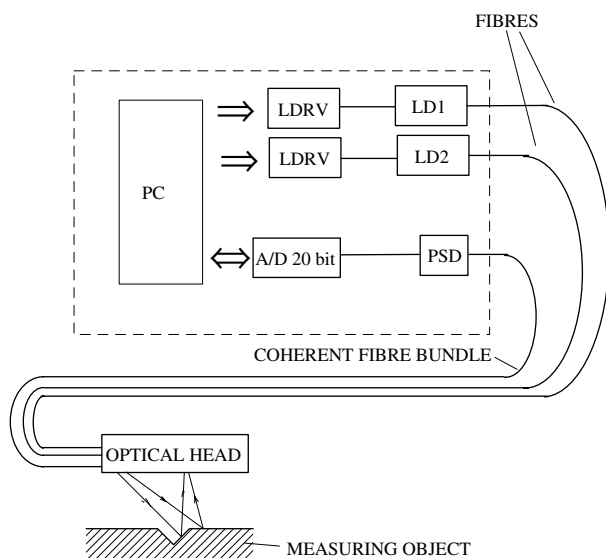


Figure 3. General arrangement of the two coordinates fibre-optic displacement sensor. (PC—personal computer, LDRV—laser driver, LD—laser diode, PSD—position sensitive detector, A/D 20 bit converter.)

5.1. The sensor head

The sensor head design is presented in figure 4. The sensor head housing is designed to hold all optical components aligned and with good mechanical stability. As there are no moving parts in the head, which could allow for subsequent alignment, the head manufacturing and assembly have to be performed with very tight tolerances. The requirement for the compact sensor head can be better understood when radiation induced activation of all materials inside the cyclotron is taken into account. The sensor head will become ‘hot’ after exposure to the cyclotron radiation and could not be touched without a health hazard to personnel. Small misalignment errors which could still exist after the head assembly can be corrected with the help of the software developed for the sensor operation allowing sensor calibration.

Careful considerations included matching the numerical apertures of used fibres and lenses.

In order to reduce the sensor head thickness, two mirrors are used to fold the beams impinging on the target and reflected from the target. This was necessary because the space available inside the dee for head mounting was only 12 mm. In that way the ‘folded’ sensor head looks at the target sideways.

In its basic design, when one-dimensional measurement is performed, optical triangulation can measure displacement of the target in the direction normal to the sensor head. With the target surface flat and parallel to the sensor head, any displacement of the target in directions parallel to the sensor head will not change the position of the laser spot on the target (relative to the sensor head) and cannot be measured. However, if one part of the target has a deliberately designed slope and the laser spot is formed on that slanted part of the target, the displacement of the target in the direction of the slope will cause a change in the position of the laser spot relative to the sensor head. This represents the basis for two-dimensional measurements. The distance from the sensor head to the flat part of the target is measured first, and then, provided the

target geometry is known, the displacement of the target in the direction parallel to the sensor head can be calculated from the position of the laser spot formed on the slanted part of the target. With a second slope formed in the direction normal to the first one, three-dimensional measurements can be performed.

5.2. Selection of fibres in the coherent bundle

A continuous light distribution on the input face of the fibre bundle, which is the same as on the target, is discretized at the output end so that the light falling on the PSD consists of discrete spots. For bundle construction we used multimode fibres, which means that any light distribution within the single fibre at the input face will be smeared out during propagation and we can expect an approximately uniform light distribution in each spot. When the fibre bundle output end is in close proximity with the PSD the light spot diameter is equal to the core diameter and spots are separated by the double value of the cladding thickness. Numerical simulation results showing the influence of a discrete fibre bundle structure on measurement error and transmission coefficient are presented in figure 5, for three types of fibres with different core/cladding diameter ratios.

The calculations have been performed for the PSD with sensitive area $3 \text{ mm} \times 1 \text{ mm}$ and the Gaussian light beam profile

$$I(x, y) = I_0 \exp\{-2[(x - x_s)^2 + (y - y_s)^2]/w^2\}. \quad (2)$$

In (2) I is the light irradiance, w is the half-width of the Gaussian beam and x_s and y_s are the coordinates of the central ray in the beam. We do not expect the beam to have a Gaussian profile in the real-life situation. This assumption is made here only for the purpose of determining the degradation of the image during relaying from one end of the bundle to the other when the light distribution at the input face is not uniform. The fibre bundle should behave similarly with other, more realistic, non-uniform light distributions at the input face, which was proven experimentally during the prototype testing.

From the diagrams in figure 5 the range of laser spot sizes with negligible measurement errors can be selected. The error becomes significant when the spot size is so small that it approaches the fibre diameter or when it is comparable to the PSD dimensions. Among the three fibres, the best choice for the coherent fibre bundle is the 110/125 fibre based on the smallest measurement error and the greatest transmission coefficient (biggest filling factor). As the end face of the optical bundle is in close proximity with the PSD surface, the differences in the numerical apertures of the different fibre types do not influence the measurement errors as there is simply no room for light to spread after leaving the fibres in the bundle.

5.3. Sensor electronics and software

The greatest errors in obtaining the PSD signal is generated using the mathematical division required by the equation in the expression (1), especially if it is performed with analogue electronic technology. The complicated analogue processing circuit required for such an operation introduces additional noise and critically degrades the overall sensor performance. Therefore, early photocurrent digitalization is performed for

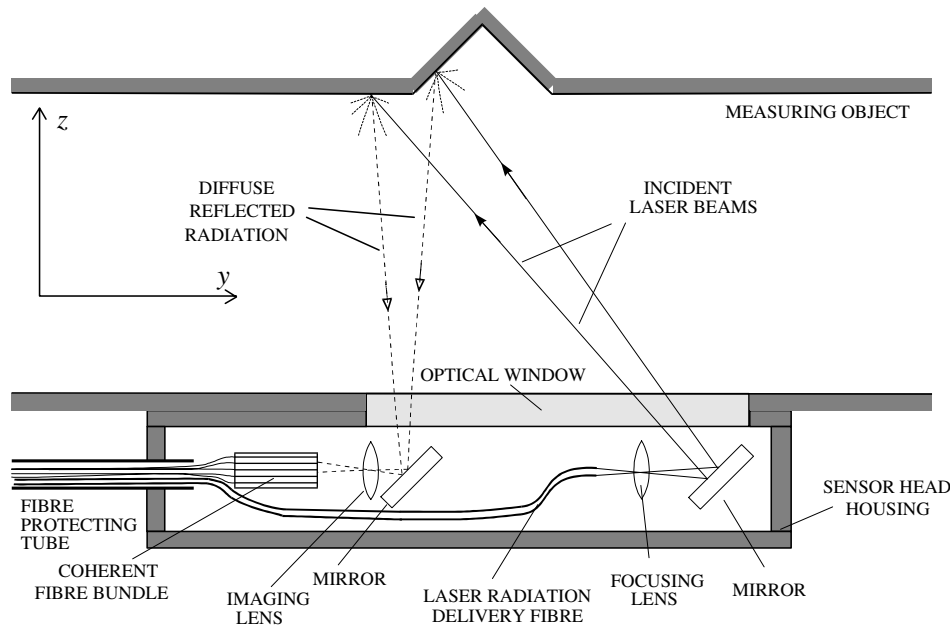


Figure 4. Optical head design for measuring two orthogonal coordinates z and y .

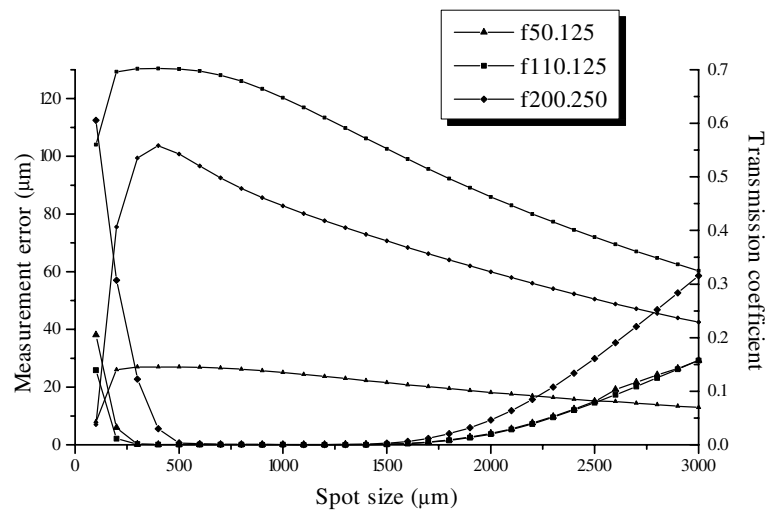


Figure 5. The influence of the coherent fibre bundle discrete structure on the measurement error and transmission coefficient for three fibres with different core/cladding diameter ratios of 50/125; 110/125; 200/250, and corresponding fill factors of 0.14; 0.68; 0.54.

both I_1 and I_2 . All the required mathematical operations can now be performed using a PC computer with greater accuracy, and there are also better possibilities of reducing the noise. The block diagram of the sensor electronics is presented in figure 6.

Burr-Brown DDC101 20-bit A/D converters are employed because they are especially appropriate for direct photocurrent digitalization. They utilize the adaptive delta modulation to provide improved noise performance and better linearity as the input signal level decreases. The DDC101 combines the functions of current-to-voltage conversion, integration, input programmable gain amplification, A/D conversion and digital filtering to produce precise, wide dynamic range results. A wide dynamic range is very important for our application because we have to start with a large optical power and still be able to perform the measurement when the radiation-induced attenuation in optical fibres become significant. DDC101 over-

sampling and digital filtering reduces system noise. Correlated double sampling eliminates offset and switching errors.

The pulsed current source for laser diodes is based on a quad operational amplifier, bipolar transistors and RC-constants. The optical output power is controlled in the feedback loop with the signal from the photodiode preinstalled in the laser diode housing.

Both A/D converters and laser power sources are connected to the PC computer through the parallel port interface. During the printed circuit board development, special care was taken to separate, as much as possible, the extremely weak analogue signals (with currents ranging from 10 pA to 500 nA) from the laser diode pulse current of 40 mA and also from the digital interfacing signals.

The system software controlled all the system components. Two laser diodes were operating alternatively; when

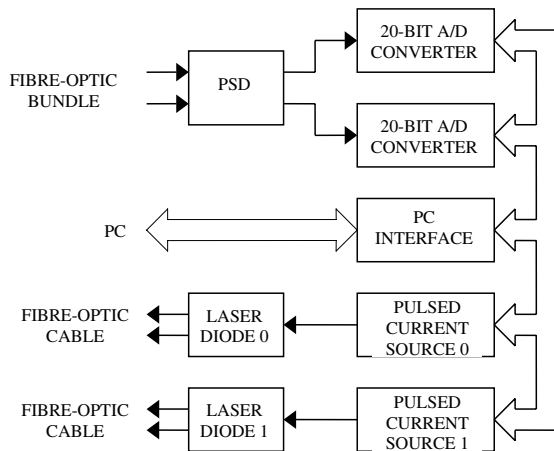


Figure 6. Block diagram of the sensor electronics.

one was on the other was off, with A/D converters synchronized with the laser diode operation. Apart from enabling the measurement of two dimensions simultaneously with one fibre bundle, this time multiplexing offered another advantage. When any of the laser diodes was off, the A/D conversion results from ambient light illumination were recorded and subtracted from the conversion results when the same diode was on, eliminating the measurement error even further.

The system software performed several more functions, ranging from the initialization procedure and self-test of all the components, to providing user menu for choice of all the setup, measuring and data-handling parameters.

6. Prototype calibration and testing

Various imperfections, such as errors in the sensor head manufacturing and assembly, lens and other optical component aberrations, defects in the fibre bundle, unknown light distribution on the input face of the fibre bundle and PSD nonlinearity, can all lead to measuring errors. Therefore the sensor has to be calibrated; this was performed with the help of a precise mechanical two-dimensional positioner.

With the first laser beam directed onto the flat surface of the target (figure 4) the distance in the z -direction, normal to the sensor head, is measured and the first calibration curve, shown in figure 7(a) is obtained. The second laser beam is directed onto the slanted part of the target (figure 4) and the signal from the PSD is recorded with the known value of the target displacement parallel to the sensor head (y -coordinate). In such a way the calibration surface shown in figure 7(b) is obtained. The calibration curve and surface presented in figure 7 are completely reproducible and they are stored in the memory of the computer. They are used as look-up tables during the measurement.

An experiment with 10 000 measurements was performed to analyse the statistical distribution of the results and evaluate the accuracy of the fibre-optic displacement sensor system. The results obey a normal Laplace–Gauss distribution (figure 8) with a standard deviation of the PSD signal that corresponds to the 20 μm movement of the target.

The 10 μm movements can be resolved with this fibre-optic sensor system. This is confirmed in the experiment in

which the target was moved in 10 μm steps. The results are shown in figure 9.

The short- and long-term stability of the system was also measured. When the system was working continuously for three days, the instability of the PSD signal was 0.001, corresponding to a 13 μm movement of the target (figure 10). We contribute this mainly to the temperature effects causing different mode distributions in multimode optical fibres and consequently different optical irradiance distribution on the PSD. We would like to point out that the magnitude of the instability, as well as the standard deviation of the PSD signal, corresponds to only a fraction of the core diameter of fibres employed in the bundle, which was 110 μm .

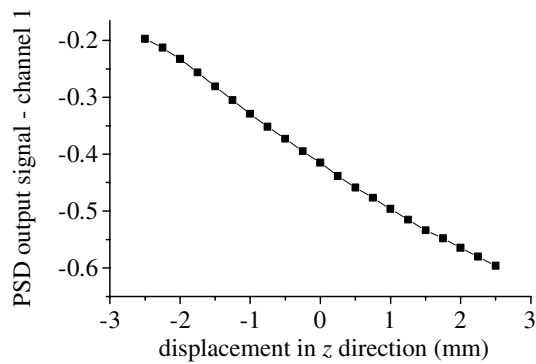
The PSD signal and the total PSD current $I_1 + I_2$ are not in correlation, as depicted from figure 10 (the correlation coefficient is -0.0678). This is proof that the PSD signal does not depend on the impinging light flux and represents a very important feature of the system, that enables the measurement accuracy to be independent of light power variations of diode lasers, variations of target reflectance, and fibre transmittance.

7. Radiation effects on optical components

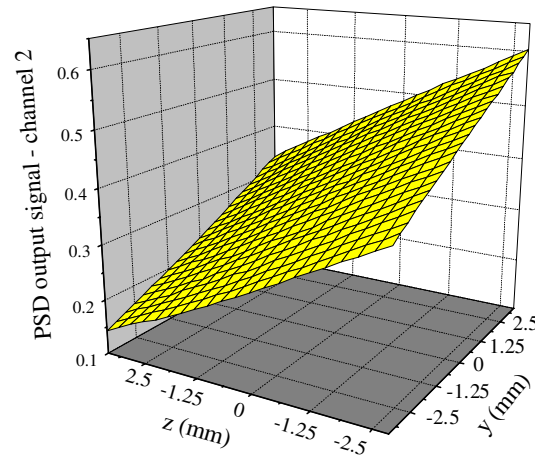
The main problem we expect in the exploitation of a fibre-optic de-position measuring system is the effect of ionizing radiation. The various energies and fluxes of neutron and gamma radiation present inside the cyclotron can affect any material with optical glass being the most susceptible. The optical head housing and lens and mirror holders are made of metal, and apart from their activation, structural changes are not expected. This is not the case with the glue usually used in the formation of optical bundles. Although the glue manufacturer could not supply any information on that matter, we suspect that the glue will completely decompose under the influence of radiation. Therefore the fibres have to be kept in their position in the bundle by mechanical means—they have to be clamped together.

The effects of radiation on glass are well known. Radiation causes defects in the glass and as a consequence so called colour centres are formed. Glass exposed to radiation becomes brown; the extent of which depends on the type and the dose of radiation. This can be catastrophic for our system because the laser light has a long path through the optical fibres exposed to the radiation inside the cyclotron. We were therefore highly motivated to search for the solution, but we were not the only ones. A lot of effort has been put in the search for radiation resistant optical fibres [25–28] because of their use in nuclear reactors.

Research on radiation-induced optical absorption shows that it is wavelength dependent, justifying the name for colour centres. It has been experimentally shown [26] that the absorption coefficient for several types of fibres does not significantly change in the wavelength region of 750–1300 nm when fibres are exposed to neutron and gamma radiation in nuclear reactors. For wavelengths smaller than 750 nm, radiation-induced absorption coefficients strongly depend on fibre core doping. The fibres with pure silica cores and with fluorine (F) doped cores are the most radiation resistant. In addition, initial structural and compositional imperfections can act as precursors for optical imperfections and will be activated by ionizing radiation to form optical absorption



(a)



(b)

Figure 7. Signals from two channels—calibration curve and surface. The target is moved in z and y directions in $250 \mu\text{m}$ steps.

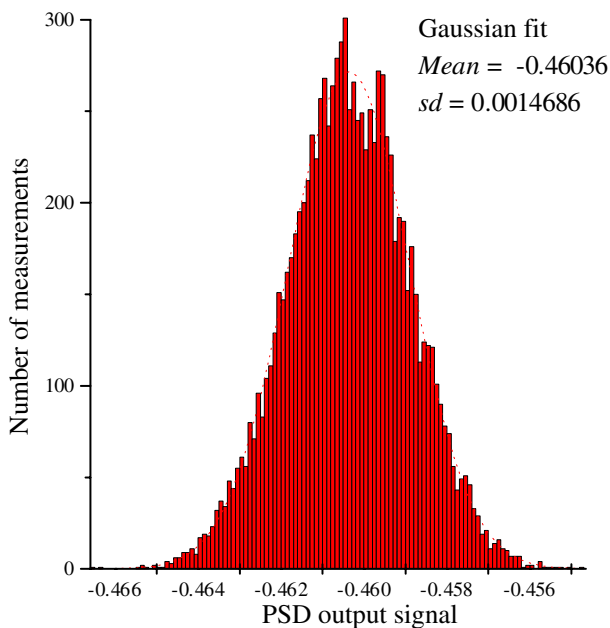


Figure 8. The statistical analysis of 10 000 measurements.

centres. Decreasing these imperfections will improve the radiation resistance of optical fibres.

It has also been shown that heat treatment, even at room temperature, can remove radiation-induced defects. At several hundred degrees the fibre recovery from defects can be complete. The heating of the fibre could be achieved by the absorption of strong laser radiation at a suitable wavelength, which will then clear its way through the fibre.

Although the energies and fluxes of neutron and gamma radiation are not the same in cyclotrons and nuclear reactors, we expect that the radiation-induced absorption in optical fibres will be similar in both cases. Several fibre manufacturers claim that they, by adequately doping and heat treating to cure structural imperfections, can produce radiation-resistant fibres for the cyclotron environment. In addition we have taken measures to prolong the useful life of a fibre by increasing to

the maximum extent possible the margin on the optical power budget. Further improvement will occur when we switch from the presently used laser diodes (with wavelengths of 680 nm , conveniently chosen for easier initial alignment) to diodes with longer operating wavelengths, where the fibre loss is smaller and the PSD silicone detector responsivity is higher.

The problem with radiation-induced absorption in the lenses and in the optical window is much less severe because the optical path length through these elements is very small and there is more experience in producing radiation resistant glass. In the sensor head, which will be placed in the cyclotron, the lenses and the optical window will be manufactured from Schott BK7G18 cerium doped glass.

When VINCY cyclotron becomes operational we intend to perform radiation resistivity studies for optical fibres in a cyclotron environment. Initially installed fibres could be replaced with more resistant ones (if such a need existed).

8. Conclusion

We presented the fibre-optic displacement sensor developed for measuring the position of electrodes of a RF cyclotron system. The sensor head is completely dielectric so that its operation will not be affected by high magnetic and RF fields inside the cyclotron. Due to its small thickness it can fit in a small space inside the electrode. All sensor electronics placement is a safe distance from the cyclotron, where the hostile cyclotron environment will not interfere with its operation.

The sensor represents completely new cyclotron diagnostics, which will help the cyclotron operator better tune the machine and avoid any electrode misalignment problems. This will improve the cyclotron efficiency and ion-beam quality.

A modified triangulation method is implemented in the sensor design, offering precision, stability, reliability, and simplicity in its operation. This sensor makes distance measurements in two orthogonal directions with a $10 \mu\text{m}$ resolution over 5 mm range. The signal from the PSD, which is employed as the sensing element, is independent of the optical flux change, so the measurement is not interfered with

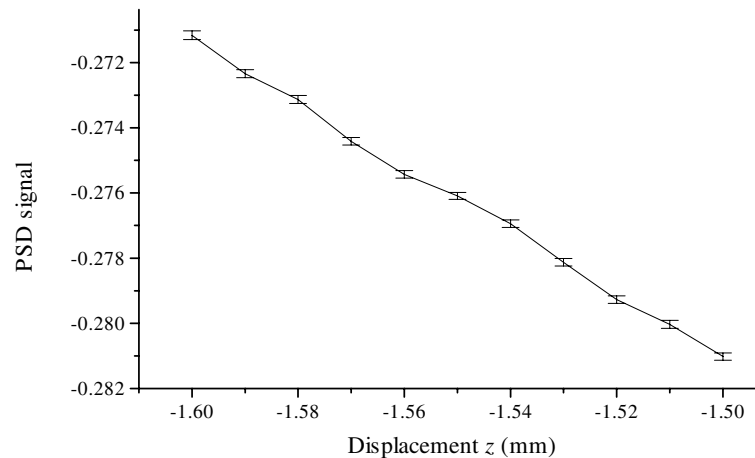


Figure 9. PSD signal versus the z coordinate. The target is moved in $10 \mu\text{m}$ steps.

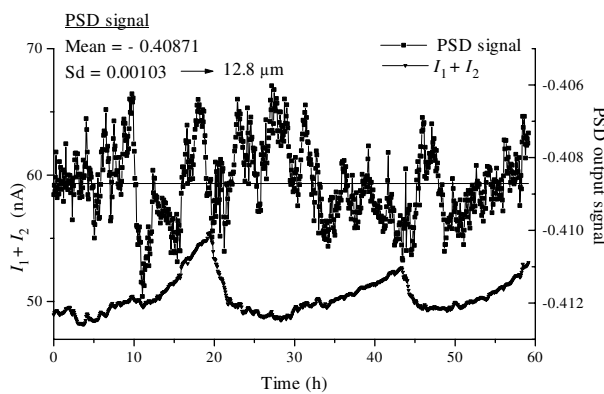


Figure 10. Three days stability measurements of the PSD sum current $I_1 + I_2$ and PSD output signal.

by any light power variation in the diode laser, any variations in the target reflectance, and fibre transmittance. This sensor system is applicable also in other hostile environments with high electromagnetic fields or ionizing radiation, such as in nuclear reactors or inside motors and generators.

Acknowledgment

We would like to thank The TESLA Centre of Excellence in Belgrade for supporting this work.

References

- [1] Blosser H G 1966 Problems and performance in the cyclotron central region *IEEE Trans. Nucl. Sci.* **13** 1–14
- [2] van Kranenburg A A et al 1966 Beam properties of Philips' AVF cyclotrons *IEEE Trans. Nucl. Sci.* **13** 41–7
- [3] Bräutigam W 1995 Beam stabilization by feedback control of the accelerating parameters in a cyclotron *Proc. 14th Int. Conf. on Cyclotron and their Applications (Cape Town, Oct. 1995)* p 280
- [4] Kilpatrick W D 1957 Criterion for vacuum sparking designed to include both rf and dc *Rev. Sci. Instrum.* **28** 824–6
- [5] Worsham R 1986 Improved reliability of the TRIUMF resonator system through installation of new resonator panels *Proc. 11th Int. Conf. on Cyclotron and their Applications (Tokyo, 1986)* p 353
- [6] Gulbekyan G G et al 1993 New development at the JINR heavy ion cyclotron facility *JINR Scientific Report E7-93-57 Dubna* p 273
- [7] Neskovic N, Vujovic V, Bojovic B, Bojovic P, Altiparmakov D, Belicev P, Maksimovic N and Dobrosavljevic A 1996 Status report on the VINCY cyclotron *Proc. 14th Int. Conf. on Cyclotrons and their Applications* (Singapore: World Scientific) p 82
- [8] Altiparmakov D, Lazovic M, Neskovic N, Morozov N A and Vorozhtsov S B 1996 Operating range of the VINCY cyclotron *Proc. 5th European Particle Accelerator Conf. vol 3* (Bristol: Institute of Physics Publishing) p 2210
- [9] Girao P, Postolache O and Faria J 2001 An overview and a contribution to the optical measurement of linear displacement *IEEE Sensors J.* **1** 322–31
- [10] Bosch T and Donati S 2001 Optical feedback interferometry for sensing application *Opt. Eng.* **40** 20–7
- [11] Beaud P, Schutz J, Hodel W, Weber H, Gilgen H and Salathé R 1989 Optical reflectometry with micrometer resolution for the investigation of integrated optical devices *IEEE J. Quantum Electron.* **25** 755–9
- [12] McGoldrick E, Beaud P, Schutz J, Hodel W, Deutsch C, Thomas N and Hubbard S A 1990 Optical characterization of arsenic-doped silica-on-silicon waveguides using femtosecond optical-time-domain-reflectometry techniques *Opt. Lett.* **15** 1354–6
- [13] Sorin W, Donald D, Newton S and Nazarathy M 1990 Coherent FMCW reflectometry using a temperature tuned Nd:YAG ring laser *IEEE Photonics Technol. Lett.* **2** 902–4
- [14] Lee C W, Peng E T and Su C B 1995 Optical homodyne frequency domain reflectometer using an external cavity semiconductor laser *IEEE Photonics Technol. Lett.* **7** 664–6
- [15] Brinkmeyer E and Ulrich R 1990 High resolution OCDR in dispersive waveguides *Electron. Lett.* **26** 413–14
- [16] Takada K, Himeno A and Yukimatsu K 1992 High sensitivity and submillimeter resolution optical time-domain reflectometry based on low-coherence interference *J. Lightwave Technol.* **10** 1998–2005
- [17] Takada K, Yamada H and Horiguchi M 1994 Optical low coherence reflectometer using (3×3) fibre coupler *IEEE Photonics Technol. Lett.* **6** 1014–16 (carress)
- [18] Takamatsu Y, Tomita K, Takagi J and Yamashita T 1990 Fibre-optic position sensor *Sensors Actuators A21–A23* 435–7
- [19] Deng K and Wang J 1994 Nanometer-resolution distance measurement with a noninterferometric method *Appl. Opt.* **33** 113–16
- [20] Tanwar L and Bansal B 1994 Sensitivity enhancement of an electro-optic sensor for displacement measurement *Opt. Eng.* **33** 1950–2

- [21] Toba E, Shimosaka T and Shimazu H 1991 Non-contact measurement of microscopic displacement and vibration by means of fibre optics bundle *SPIE Fibre Opt. Laser Sensors IX* vol 1584 pp 353–63
- [22] Culshaw B and Dakin J 1989 *Opt. Fibre Sensors: Systems and Applications* vol 2 (Norwood: Artech House)
- [23] Zivanovic S, Elazar J and Tomic M 1997 A fibre-optic position sensor for non-contact measurement in hostile environment *Proc. 10th Annual Meeting IEEE Lasers and Electro Optics Society LEOS'97* (San Francisco, USA, Nov. 1997) vol 2 pp 562–3
- [24] Hamamatsu—large-area PSD series catalog available at <http://www-cdr.stanford.edu/MADEFEST/catalogs/hamamatsu/psd-principle.html>
- [25] Tomashuk A L and Golant K M 2000 Radiation-resistant and radiation-sensitive silica optical fibres *Advances in Fibre Optics (SPIE vol 4083)* pp 188–201
- [26] Shikama T, Kakuta T, Shamoto N, Narui M and Sagava T 2000 Behaviour of developed radiation-resistant silica-core optical fibres under fission reactor irradiation *Fusion Eng. Design* **51–52** 179
- [27] Kakuta T, Shikama T and Shamoto N 1999 Development of radiation-resistant optical fibres for visible application *Proc. SPIE* **3872** 11
- [28] Gurzhiev A N, Turchanovich L K, Vasilchenko V G, Bogatyryev V A and Mashinsky V M 1995 Radiation hardness study of optical fibres *Report IHEP 95-121* (Moscow: Institute For High Energy Physics)